Remotely Sensing Digital Methods For Dust Storms Monitoring In Iraq

Mustafa Ali Hassan*
Unit of Remote Sensing, College of Science, University of Baghdad, Baghdad, Iraq

Abstract

In this research, attempt to overcome and quantities the problem of the large number of frequency of dust storms and the areas that generated and then identifying these areas in order to be held by the agricultural areas, as has been the adoption of many of the techniques and methods of processing image in remote sensing and geographic information systems and linking them together to identify those areas in Iraq or the neighbors, especially the northern and north-west wind of the fact that Iraq is in the northern and north - western most days of the year. Research has included the use of images from the satellite (MODIS) with quality (Aqua) and (Terra) with the assembly of the amount of dust, these storms, it was determining the values of size and density of the dust and the amount (> 10μm) and (ρ = 1.58 mg/m3) respectively, note that this dust has collected from the University of Baghdad during a sandstorm brief summary on July 2010, because this month is the most higher month temperature in the year and it was about 50 thousand ton of dust in each dust storm. To extract all the results and information that obtained from the operations account amounts that the soil is expected calculated annually for these storms and to determine the threshold line density of this dust in the air. Finally, developing a system to monitor these storms, depending on the capacity of scientific instruments of modern used in the countries of the world and its establishment in Iraq.

طرق استشعار عن بعد رقمية لمراقبة العواصف الترابية في العراق

مصطفى علي حسن
وحدة الاستشعار عن بعد، كلية العلوم، جامعة بغداد

الخلاصة:

في هدا البحث تم دراسة مشكلة العدد الكبير من العواصف الترابية ومناطق نشأتها وأيجادها. حيث أن هده المناطق تؤثر بشكل كبيرعلى المساحات الزراعية وتم أستخدام العديد من تقنيات وطرق معالجة الصور الرقمية في التحسس النائي و نظم المعلومات الجغرافية والربط مابين هده الطرق والتقنيات لأيجاد هده المناطق ومساحاتها في العراق بشكل خاص .بصورة خاصة فأن الرياح في العراق في معظم أيام السنة هي رياح شمالية وشمالية–غربية . تضمنت الدراسة أستخدام صور فضائية رقمية للقمر(MODIS)دو نوعية (Aqua), (Terra)لنمدجة الغبارفي هده العواصف حيث تم دراسة الحجم والكثافة والتي كانت (ρ = 1.58 mg/m3) and (> 10μm)حيث تم جمع النمادج في جامعة بغداد خلال العواصف الترابية في شهر السابع شهر تموز بسبب أن هدا الشهر هو ألأكثر أرتفاعآ لدرجات الحرارة والعواصف الترابية في هدا الشهر جهزت غبار حوالي 50000 طن من الغبار وتم تحديد مناطق نشأت هده العواصف في العراق.

Introduction

Remote Sensing is the science and art of obtaining information about an object area or phenomenon through the analysis of data acquired by a device that is not in contact with the object, area, or phenomenon under

*E-mail: dr.musstafaalneamy@yahoo.com

investigation. The three most common types of platform for atmospheric remote sensing are (ground based, aircraft and satellites). For large phenomena usually used satellites. The dust storms consider very large phenomena dust storm, a general name of sand storm and dust storm, is the weather condition which means strong wind draws much sand and dust near the ground surface into the sky, making air very foul, causing visibility less than 100 meter. It is a complex process influenced by the interaction of earth-atmosphere system, mainly caused by high wind speed, bared soil and dry air condition etc. It often takes place in arid and semi-arid areas. In recent years, the frequency of dust storm is rising. Dust storm can impact the climate changes and cause great damage to people. It is very necessary to monitor the disasters timely and accurately, In recent years, The frequency of dust storm is rising, and occur in many parts of the world [1,2], especially in the Middle East, Africa and arid parts of Asia, as well as in the north west and south west of the Iraq (the region of interest of the study), A "dust or sand storm" is a meteorological phenomenon caused by severe weather conditions, specifically dry area with high surface winds which pick up loose dust. Severe dust storms can reduce visibility to zero. The average height of a dust storm it can extend far into the atmosphere is from about (900m to 1800m) or even higher in the mid troposphere. The images (as shown in figure 1-, 2- illustrate the severities of dust storms in the dry states, such as Middle East and Iraq. Much of this dust is propagated out of the region by the upper-level winds. Summer wind maximum in the mid troposphere, is imbedded in the Sahara dust layer. Due to its strength and stability, moves dust as far as the original region of the beginning . It represent serious natural hazards. Dust storm can impact the climate changes and cause great damages to people health, agriculture, ground transport and the microwave signal attenuation caused by dust. D.S. is one of the major problems in utilizing microwave bands for terrestrial and space communication especially at desert and semi desert. Dust storm detection and tracking could be difficult as they share some similar characteristics to clouds. Dust storms can vary in their shape, particle size, and distribution; hence normally show a varying behavior, [2]. The daily observations of aerosol from satellites over land and oceans are required to obtain a global aerosol budget, monitor aerosol sources, and transport chemical transformation in the atmosphere and sinks. This information can then be used to evaluate the aerosol radioactive forcing of climate, [3]. And the climatic response to the presence of troposphere aerosol, [4]. Aerosols are characterized by high temporal and spatial variability, due to their short lifetime of a few days, [5]. Thus, satellites are suitable to monitor this variability. Several satellite sensors are designed to measure global aerosol concentration and properties using the spectral, angular, or polarization properties of solar radiation reflected by the aerosol The spectral properties are used by the Earth observing system-moderate resolution imaging Spectroradiometer (EOS-MODIS) [6,7] and the Advanced Earth observing system–ocean color and temperature scanner (ADEOS-OCTS) and Global Imager (GLI) sensors, [8]. The angular characteristics are by EOS-Multi-Angle Imaging Spectral Radiometer (MISR) [9, 10], and ADEOS-Polarization and Directionality of the Earth's Reflectance (POLDER) and the Polarization Measurements also by (POLDER) [11,12].

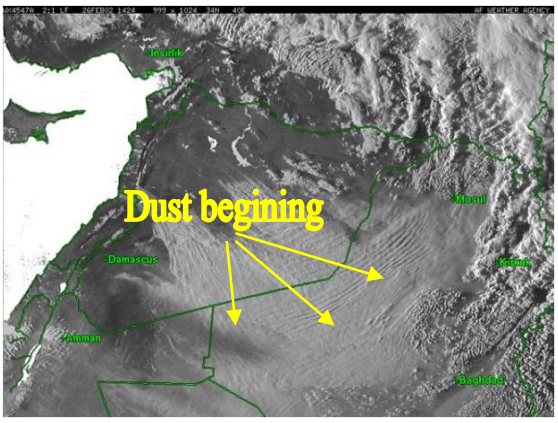

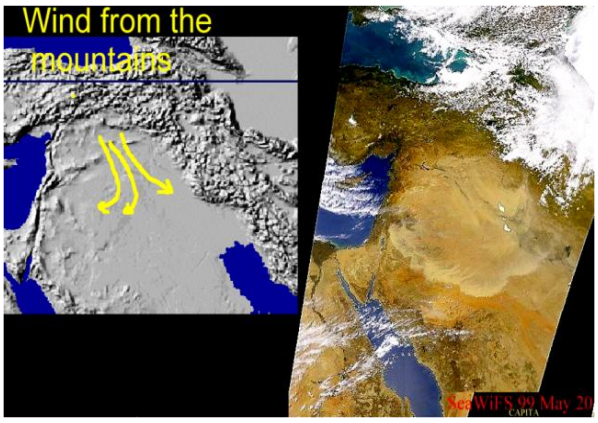

Figure 1-A, the big dust storm in Iraq in 20-05-1999, B graphic for the dust storm[13]

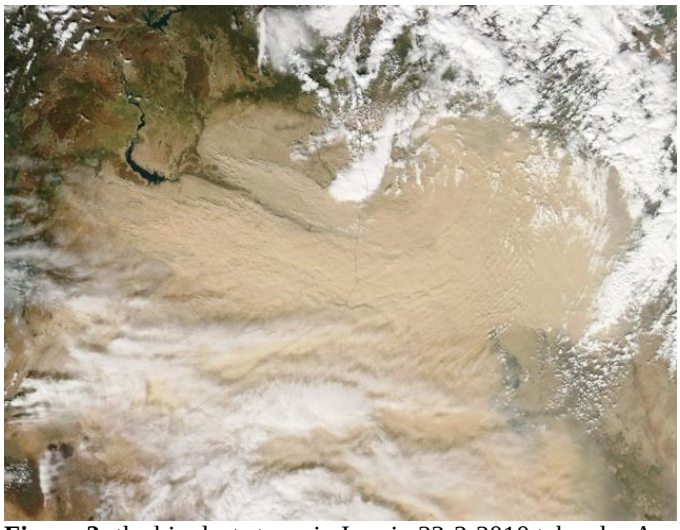

Figure 2- the big dust storm in Iraq in 22-2-2010 taken by Aqua and terra

Monitoring Of Dust Storms By Remote Sensing Methods

Remote sensing has shown to be a valuable tool in detecting, mapping and forecasting . It is very necessary to monitor the disasters timely and accurately. Weather condition which means strong wind draws much sand and dust near the ground surface into the sky, making air very foul. Its content in air is less than 0.1 mm and is called dust and above that it is called sand. SDS is a complex process influenced by the interaction of earth-atmosphere system, mainly caused by high wind speed, bare soil and dry air condition, [1]. It often takes place in arid and semi-arid areas. This research used the Moderate Resolution Imaging Spectroradiometer (MODIS), Two MODIS instruments, the first launched on Dec. 1999 onboard the Terra (previously known as EOS AM-1) satellite. The second MODIS was launched onboard the Aqua (EOS PM-1) satellite in May 2002. MODIS senses all the Earth's surface in 36 spectral bands spanning the visible (0.415 μm) to infrared (14.235 μm) spectrum at nadir spatial resolution of 3 modes (1 km, 500 m and 250 m). The associated remote sensing applications are of interest not only to land, ocean, and atmosphere discipline researchers but also to application, interdisciplinary and environmental scientists . The MODIS instruments are carried aboard the Earth Observing System (EOS) Terra and Aqua polar orbiting satellites. The high spatial and spectral resolution of MODIS enhances the visibility of airborne dust over land and water, allowing for detailed analysis of dust activity at selected hotspot areas The MODIS sensor on AQUA and Terra can provides 250m resolution images of the dust storm in free at the web site, http://www.modis.gsfc.nasa.gov.. A digital color image displayed on a monitor is composed of three different color channels: red, green, and blue. Satellite images are made by combining the reflected light detected by the sensor at various wavelengths (spectral bands) and making them into a single image. The MODIS Rapid Response System makes use of MODIS broad range of spectral observations by creating both true-color and false-color images, each tailored to highlight different land surface, atmospheric, and oceanic features. Some of the ways these bands can be combined are described below. Normalized Difference Dust Index (NDDI) can be used to eliminate the influence of cloud and snow effectively. The NDDI can be written as:-[2].

$$\mathrm{NDDI} = \frac{(b7-b3)}{(b7+b3)} \quad \ldots\ldots\ldots\ldots\ldots\ldots (1)$$

where b3,b7 are reflection at the third band and the seventh band of MODIS, [4,13].

Normalized Difference Dust Index (NDDI)

Several indices have been proposed based on the spectrum characteristics, proposed the Normalized Difference Water Index (NDWI) for monitoring vegetation water content with the (0.86 μm) band and either the (1.64-μm) band or the (2.13-μm) band, [14]. The spectral characteristic of sand suggests that strong SDS signals can be obtained using the difference between the (2.13-μm) band signal, which is high, and the (0.469-μm) band, where the signal is relatively much lower. This difference distinguishes rather well between SDS and water or ice clouds. Because of this strong discrimination possibility, it is propose an NDDI to detect SDS. The NDDI can be shown in figure 3- and written as, [13, 14]

NDDI = (ρ2.13μm − ρ0.469μm)/(ρ2.13μm + ρ0.469μm)……. (2)

where (ρ2.13μm) and (ρ0.469μm) are reflectance at the top of atmosphere (TOA) in the (2.13- μm) and (0.469-μm) bands, respectively. To investigate the feasibility of NDDI for detecting SDS, there is nine cases of SDS over the Gobi region and analyzed the NDDI ranges of dust, cloud, and surface features. For clouds, the NDDI value is negative (NDDI < 0.0) because of the higher reflectance at the (0.469-μm) band and lower reflectance at the 2.13-μm band,[14]. There are many instruments to calculate the density, direction, high, etc. of dust in air and atmosphere such as taking data from the (AREONET) (Aerosol Robotic Network) program which is a federation of ground-based remote sensing aerosol networks established by NASA and PHOTONS (Univ. of Lille 1, CNES, and CNRS-INSU) and is greatly expanded by collaborators from national agencies, institutes, universities, individual scientists, and partners. The program provides a long-term, continuous and readily accessible to public domain database of aerosol optical, microphysical and radioactive properties for aerosol research and characterization, validation of satellite retrievals, and synergism with other databases. The network imposes standardization of instruments calibration, processing and distribution. Aerosol Robotic Network (AERONET) collaboration provides globally distributed observations of spectral Aerosol Optical Depth (AOD), inversion products, and perceptible water in diverse aerosol regimes. Aerosol optical depth data are computed for three data quality levels: Level 1.0 (unscreened), Level 1.5 (cloud-screened), and Level 2.0 (cloud-screened and quality-assured). Inversions, perceptible water, and other AOD-dependent products are derived from these levels and may implement additional quality checks. The processing algorithms have evolved from Version 1 to Version 2.0 (fully released in July 2006) and are available from the AERONET and PHOTONS web sites. Version 1 data may be downloaded from the web site through 2006 and thereafter upon special request. New AERONET products will be released as new measurement techniques and algorithms are adopted and validated by the AERONET research community, http://aeronet.gsfc.nasa.gov.

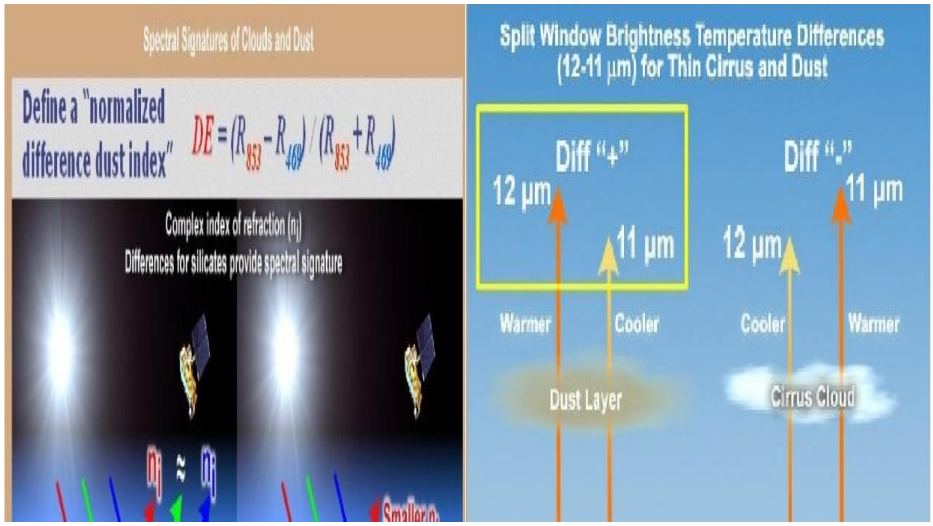

Figure 3- the define of NDDI between two bands, A, on clouds, B, reflected on earth surface, http://aeronet.gsfc.nasa.gov.

Point Sources of Dust

The image shows in figure 4- source regions for dust, marked with yellow dots, in the Middle East. Note that this figure identifies small areas as source regions. This is because it turns out that Most of the dust comes from a number of discrete areas. These areas are small enough, compared to the plumes they generate, that they can be regarded as point sources, much like a smokestack,[15,16].

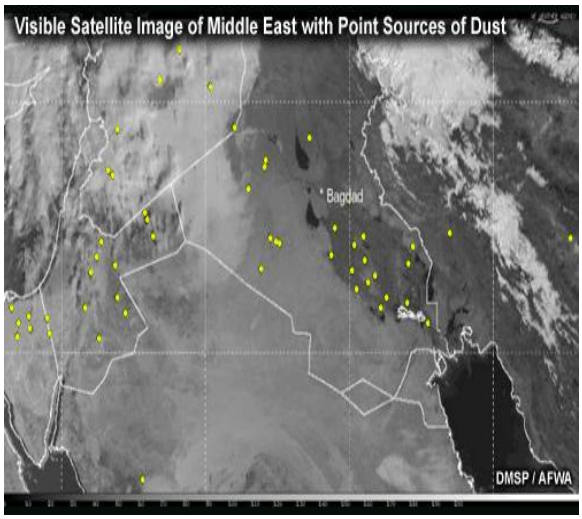

Figure 4- the area of the source dust in middle east,[13 ,16].

Method and Analysis

It is very necessary to monitor the disasters timely and accurately. At present, the ground based measurement method and remote sensing technology are two main methods for monitoring dust storm. When dust storm happens, the environmental condition is often very bad. The sites for measuring dust storm are usually laid sparsely. As a result, because of low temporal and spatial resolution, traditional ground based measurement method cannot meet the requirements of dust storm monitoring and forecasting very well. The technology of satellite remote sensing has many advantages, such as: wide coverage, continuous in the space and monitoring natural disasters quickly, so it can act as an important role in the dust storm monitoring. Remote sensing can monitor the scope of dust storm, its intensity grade and its moving trace .

MODIS Interdiction Bands

The data used to monitor dust storm disaster is MODIS data. MODIS has three different spatial resolutions including 250 m (bands 1–2), 500 m (bands 3–7), and the 1-km (bands 8–36) and the Swath width 2330 Km Cross-track scanning. There are a total of 20 solar reflectance bands (SRBs) (1–19 and 26) from (0.41–2.13 μm), [3, 19], MODIS sensors, boarded on both Terra and Aqua satellites, have 36 channels. Its spectrum ranges is (0.4 um ~ 14.385 um), covering from visible to infrared. At least 4 MODIS images can be obtained every day. The timeliness of data is increasing, so dust storm can be monitor dynamically.

MODIS Data Collection And Processing

To develop a robust approach for dust detection using MODIS TIR bands, sufficient measurements and delicate analysis are essential. Major dust events over this region was identified between the past 3 years, i.e. 2004-2006, and collected the corresponding MODIS L1B calibrated radiance (1km), MODIS L1A geolocation, and MODIS L2 aerosol data products for analysis and testing. The times of the selected MODIS granules are listed in Table 1- For each granule in Table 2-, MODIS brightness temperature is calculated from the 1 KM calibrated radiances (L1-B) data and aggregated to 10 km resolution. Then the brightness temperatures at 10km resolution and MODIS AOT at 550nm over ocean are merged into a negative values because of cloud or retrieval failure. These invalid data are filtered out in our study. The final database contains 191762 records of MODIS brightness temperature and AOT at 10 km resolution, [17].

Modis Band Selection

The sensitivity of thermal infrared bands to dust was studied and was found that brightness temperature difference between(3.7μm and 12μm), and brightness temperature differences between (11μm and 12μm) were sensitive to dust storms . The brightness temperature difference between (11 μm and 12μm) has been widely used to differentiate dust from other aerosols and cloud. In this study, four MODIS bands, i.e., band 20, 30, 31, and 32 were selected for dust detection and analysis. 31, and 32, respectively.[17,18].

Table 1- MODIS granules collected for dust storm detection and analysis

Band	Bandwidth
20	**3.660 -- 3.840 μm**
30	**9.580 -- 9.880 μm**
31	**10.780 -- 11.280 μm**
32	**11.770 -- 12.270 μm**

Table 2- MODIS thermal IR bands used for dust detection

Satellite	Time (Julian day, UTC)
Aqua	**2004064, 14:55, 15:00**
Aqua	**2004065, 14:00, 14:05**
Aqua	**2004066, 14:40, 14:45, 14:50**
Aqua	**2004067, 13:55, 15:30**
Aqua	**2004068, 14:30, 14:35**
Aqua	**2004204, 13:45, 13:50**
Aqua	**2005001, 14:15**

Terra	**2005007, 12:10**
Terra	**2005043, 11:45**
Aqua	**2005043, 14:50, 14:55**
Terra	**2005136, 11:15, 11:20, 12:55**
Aqua	**2005136, 14:20**
Aqua	**2005139, 14:50**
Terra	**2005139, 11:45, 11:50**
Terra	**2005200, 11:15**
Aqua	**2005200, 14:20**
Terra	**2005227, 10:55**
Aqua	**2005227, 14:05**
Terra	**2005247, 12:10**
Aqua	**2005227, 15:15**
Terra	**2006067, 12:05**
Aqua	**2006067, 13:35, 15:10**

The PCA Methods Dust Change Detection (Mathematical Description)

The principal components transform can be visualized most easily in two-1dimensional, shown in figure 5- . Let a two- dimensional distribution of pixel values obtained in two bands, labeled simply by X1 and X2. A scatter plot of all the brightness values associated with each pixel in each band is shown in figure (5-a) together with the locations of their means µ1 and µ2. The goal is of the PCA to translate and / or rotate the original axes so that the original brightness values on axes X1, X2 are redistributed onto a new set of axes or dimensions, X1´, X2´. For example, the simple translation for the original data points from X1 to X1´ and from X2 to X2´ coordinates system might be the relationship;

$X_1' = X_1 - \mu$ and $X_2' = X_2 - \mu_2$……. (3)

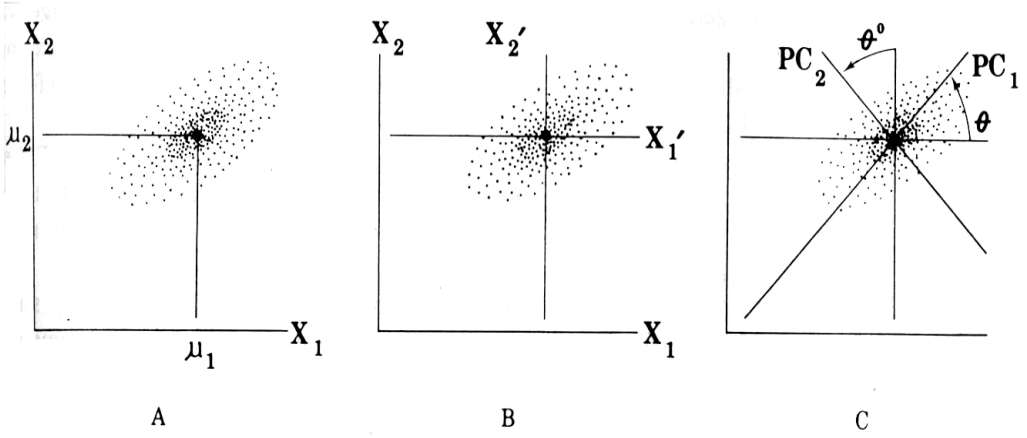

Figure 5- the Two- Dimensional (PCA) Transform

The origins of the new coordinates now lies at the location of both means in the original scatter of points, figure 5b-, The new coordinates system might then be rotate about its new origin (μ_1, μ_2) in the some θ degrees so that the first axis X_1' is associated with the maximum amount of variance in the scatter plot of points, figure 5c-, This new axis is called the first principal components (PC1=λ1). The second principal components (PC2=λ2), is perpendicular (orthogonal) to PC1. Where λ1, λ2 are the transformation's Eigen values. The major and minor axes of the ellipsoid of points in bands X1, X2 are called the principal components. To transform the original data on the X1, X2 axes into the PC1 and PC2, we must obtain cretin transformation coefficients that we can apply in a linear fashion to original pixel values. The linear transformation requires a derivation from the covariance matrix of the original data set.

The mathematical procedures involved the following two-dimensional "PCA" transformation,. Consider a set of multi-band images f(x, y, r), each of size M×N and "r" bands.

1. Each image band should be expressed in the form of an n-dimension vector Dn,1, where n = M×N, given by, [20]:

$$D_{n,1} = \begin{bmatrix} f(1,1,1) \\ f(1,2,1) \\ \cdot \\ \cdot \\ \cdot \\ f(i,j,1) \\ \cdot \\ \cdot \\ f(N,M,1) \end{bmatrix} \quad \text{..... (4)}$$

The whole image bands are, then, arranged into a matrix $D_{n,r}$ of n-rows and r-columns, given by, [20]:

2. The mean of each column in equation (4) should be computed by taking the arithmetic averages of each column, given by:

$$\bar{D}_{n,b} = \frac{1}{n}\sum_{i=1}^{N}\sum_{j=1}^{M} f(i,j,b), \text{ where b=1,2,....,r} \quad (5)$$

3. An (n-row, r-column) matrix $P_{n,r}$ is computed by subtracting the mean of each column $\bar{D}_{n,b}$ from that column values $D_{n,b}$. This matrix is called the "Mean-Corrected-Data-Matrix", its values are given by:

$$P_{j,b} = \sum_{i=1}^{n}(D_{i,b} - \bar{D}_{i,b}),\ j = 1,2,...,n \text{ and } b = 1,2,.....,r \quad (6)$$

4. The covariance matrix of the $P_{j,b}$ matrix can then be computed by:

$$C_P = E\{(D-\bar{D})(D-\bar{D})^T\} \quad (7)$$

Where E{.} is the expectation operation, "T" indicates transposition, and C_P is an r×r matrix.

5. Now, assume that e_i and λ_i, for i=1,2,3,……n, be the eigenvectors and corresponding Eigen values of the matrix C_P. For convenience, we shall assume that the Eigen values being arranged in decreasing order, such as, $\lambda_1 \geq \lambda_2 \geq \lambda_3 \ldots \geq \lambda_n$.

6. A transform matrix" A" whose rows are the eigenvectors of C_P can should, then, be computed, given by:

$$A = \begin{bmatrix} e_{11} & e_{12} & e_{13} & \cdots & e_{1n} \\ e_{21} & e_{22} & e_{23} & \cdots & e_{2n} \\ \vdots & & & & \\ e_{n1} & e_{n2} & e_{n3} & \cdots & e_{nn} \end{bmatrix} \quad \ldots\ldots\ldots \quad (8)$$

7. The principal components vectors can, now, be computed by utilizing the transformation:

$$Y_i = A(D_i - \bar{D}_i),\ for\ i = 1,2,3,....,r \quad (9)$$

$$D_{n,r} = \begin{bmatrix} f(1,1,1) & f(1,1,2) & \cdots & f(1,1,r) \\ f(2,1,1) & f(2,1,2) & \cdots & f(2,1,r) \\ \vdots & \vdots & \cdots & \vdots \\ f(i,j,1) & f(i,j,2) & \cdots & f(i,j,r) \\ \vdots & \vdots & \cdots & \vdots \\ f(N,M,1) & f(N,M,2) & \cdots & f(N,M,r) \end{bmatrix}$$

In fact, the transformation presented in equation (9) has several important properties, these are:

- An inverse transformation operation can be performed by.

$$D_i = A^{-1}Y_i + \bar{D}_i \quad (10)$$

Since C_P is a real, symmetric matrix, it is always possible to find a set of orthogonal eigenvectors, which yield $A^{-1} = A^T$.

- Instead of using all the eigenvectors of C_P, we can form A_K^T from only K-eigenvectors, corresponding to the largest Eigen values λi.
- The Yi vectors will then be K-dimensional and the reconstruction will no longer be exact, i.e.

$$\hat{D}_i = A_K^{-1} Y_i + \bar{D}_i,\ for\ i = 1,2,3,...,K \quad (11)$$

The experimental work can be found in Chapter four to find the change detection for tow images,[22].

Experimental work and results

In this section, the experimental work and results analysis will introduce, which include, registration processes (image to map), classification, methods of dust detection, calculation of dust storm area, and find the weak areas that generate the dust storms. The data used to monitor dust storm disaster is MODIS data. MODIS sensors, boarded on both Terra and Aqua satellites. The images spectrum range was (0.4μm-14.385μm), covering the spectrum from visible to infrared. At least 4 MODIS images can be obtained every day. As the timeliness of data is increasing, so dust storm can be monitored dynamically, but these images must purchase from the site. Therefore, the free images on the MODIS site include manly visible bands that can be used with spatial resolutions (1Km, 500m, and 250 m) three bands. The table 3- show the band used to detect the dust storms**,** [17]. The images that can be collect from the MODIS website were of extension (JPG), with 3-bands only with varies spectral regions, therefore, they must rectify in order to used for any application. The rectification process that used was image to map correction of first order polynomial, table 3- represent the spectral bands of MODIS system.

Table 3- MODIS Bands Used in dust Detections, [15]

Channel	λ(mm)a	Resolution (km)	Description
B1-1b	0.645	0.25	Red
B2-2b	0.853	0.25	Reflective IR
B3-3b	0.469	0.50	Blue
B4-4b	0.555	0.50	Green
B5-26	1.38	1.0	Shortwave Vapor
B6-31	11.0	1.0	IR Window 1
B7-32	12.0	1.0	IR Window 2

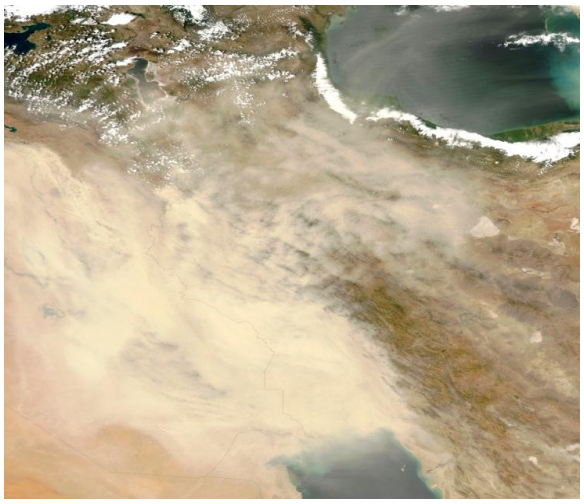

Figure 6- the Input dusty Image(5/7/2009)

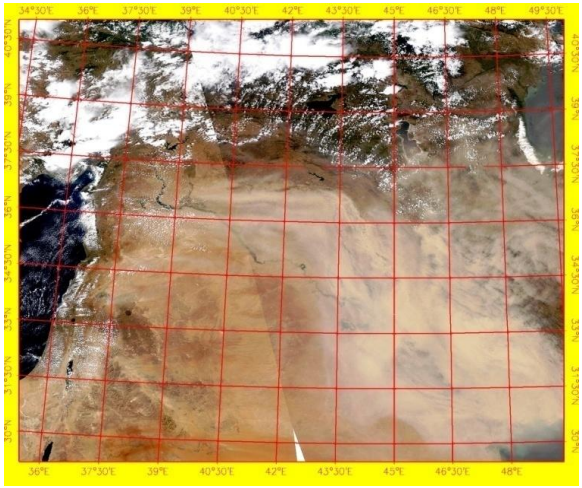

Figure 7- the Geo-Reference dusty Image (5/7/2009)

Particle –Size Distribution Test:

The sample was calculated from residual of dust storm at Baghdad Al-government in 13/8/2009, and conducted the sieve and hydrometer analysis tests in soil investigation Labs (NCCLR) /Baghdad, according to requirements of ASTM-422-68 (Re approved -1998) and the results are presented in Figure 8-, which included the following;

- The sizes range between (0.003 – 0.16) mm
- The effective size (D_{10}) was = 0.0063 mm
- The coefficient of uniformity =7.46
- The coefficient of graduation = 1.09

The test sample can be describe as well graded Silt (80%) with little fine sand (12%) & clay fraction (8 %). From above results, it can classify that the type of dusty storm and the particles are small enough to stay lifting by currents of turbulent air in the space of Baghdad as suspension. The effective size of a given sample of sand is the particle size (in millimeters) where 10% of the particles in that sample (by weight) are smaller, while 90% are larger. Usually this is denoted as the D10.

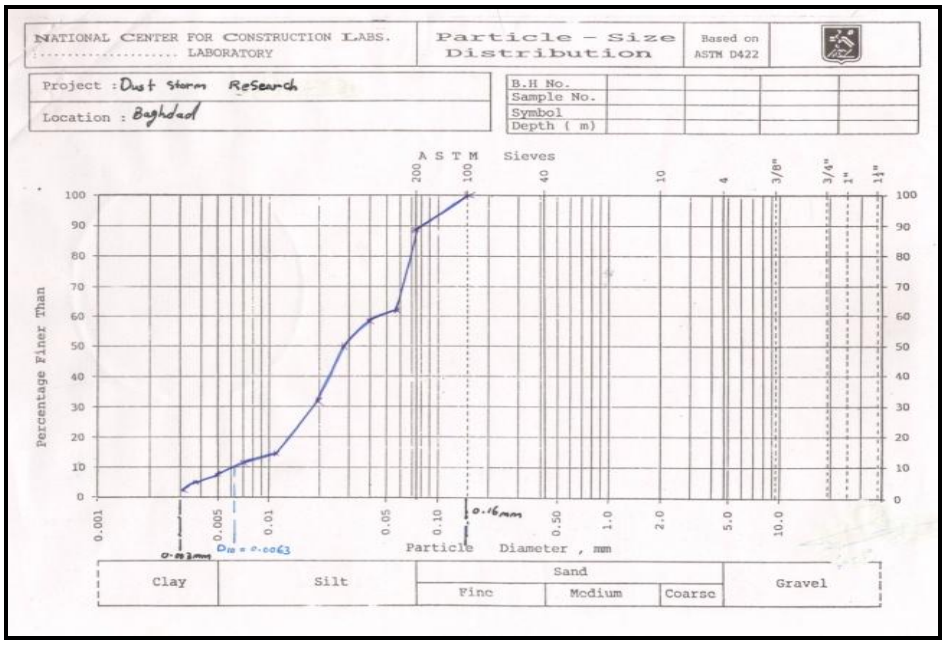

Figure 8- Particle Size Distribution Test

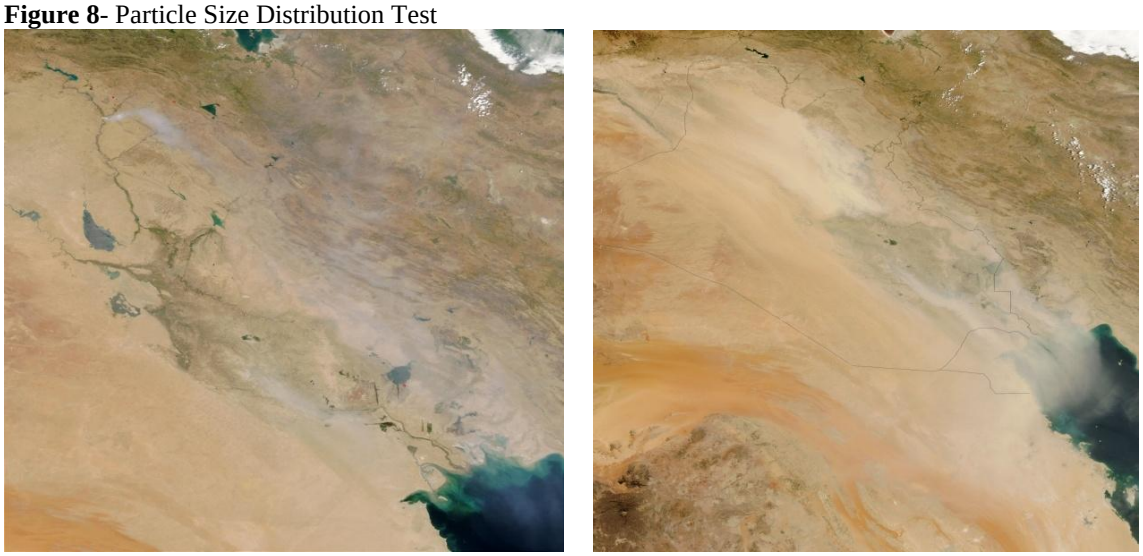

Figure 9- the MODIS Aqua (EOS PM) Satellite Temporally Images, Visible Bands, 500 m Spatial Resolution

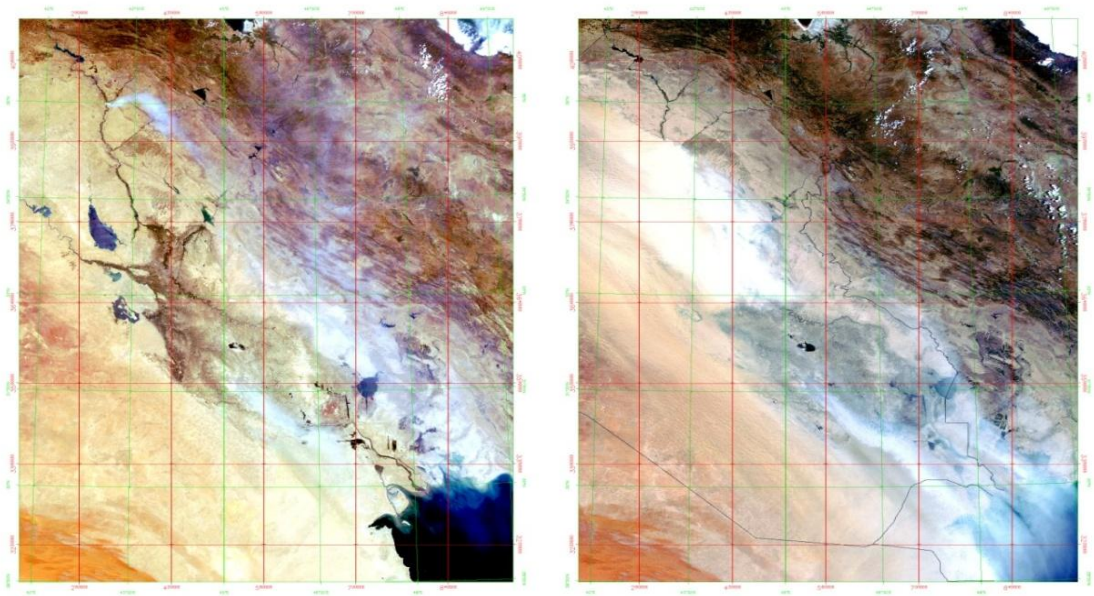

Figure 10- the Geo-Match, First & Second Images Respectively

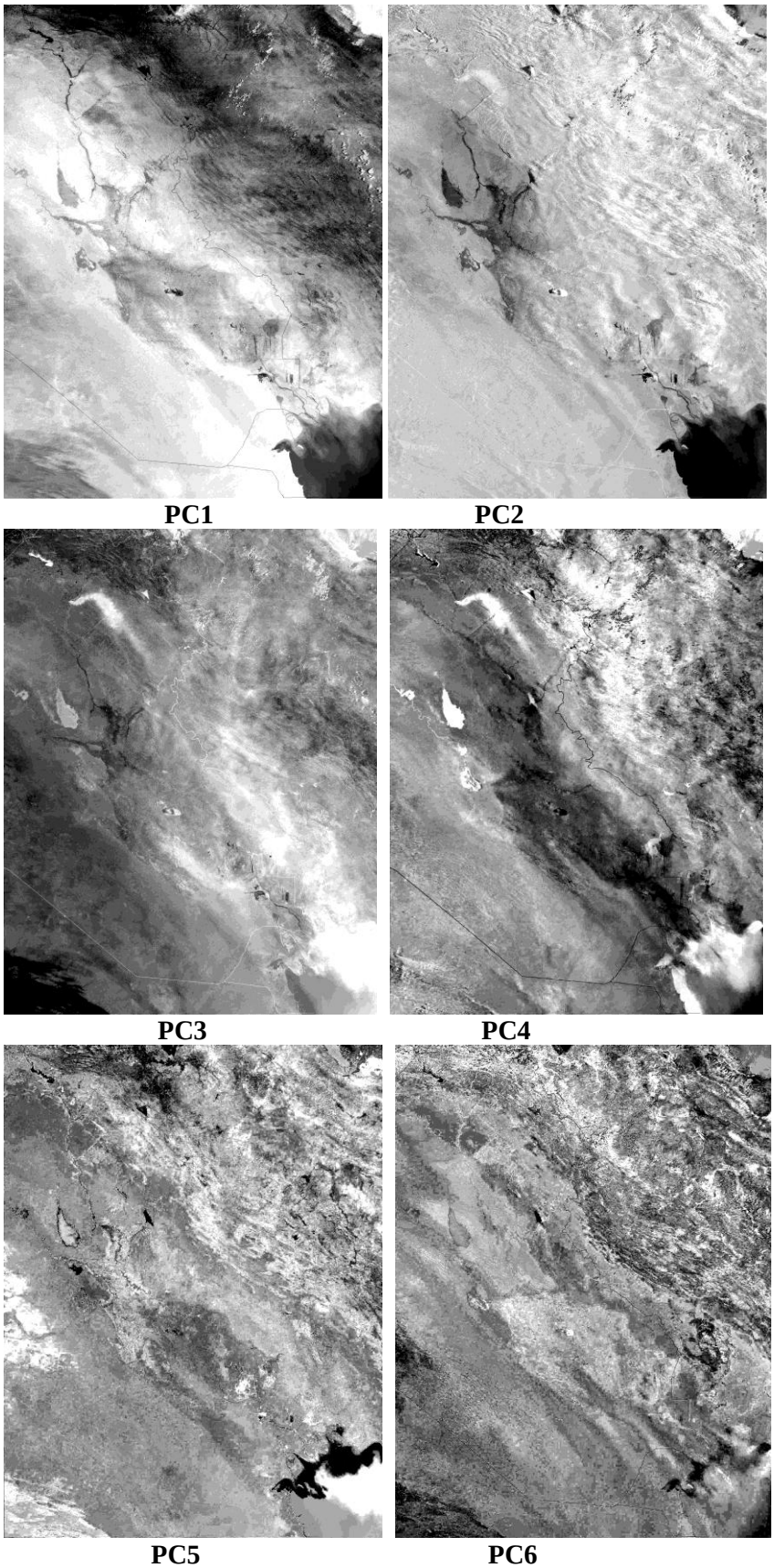

Figure 11- the 6 PCs For The Geo-Matched Temporally Images

The Eigen values of the PCs was indicate the table 4- .

Table 4- The Eigen Values Resulting From PCA Kernel, ENVI, v4.5

Eigen Values of The 6 PCs					
PC1	**PC2**	**PC3**	**PC4**	**PC5**	**PC6**
0.63	**0.27**	**0.05**	**0.02**	**0.017**	**0.013**

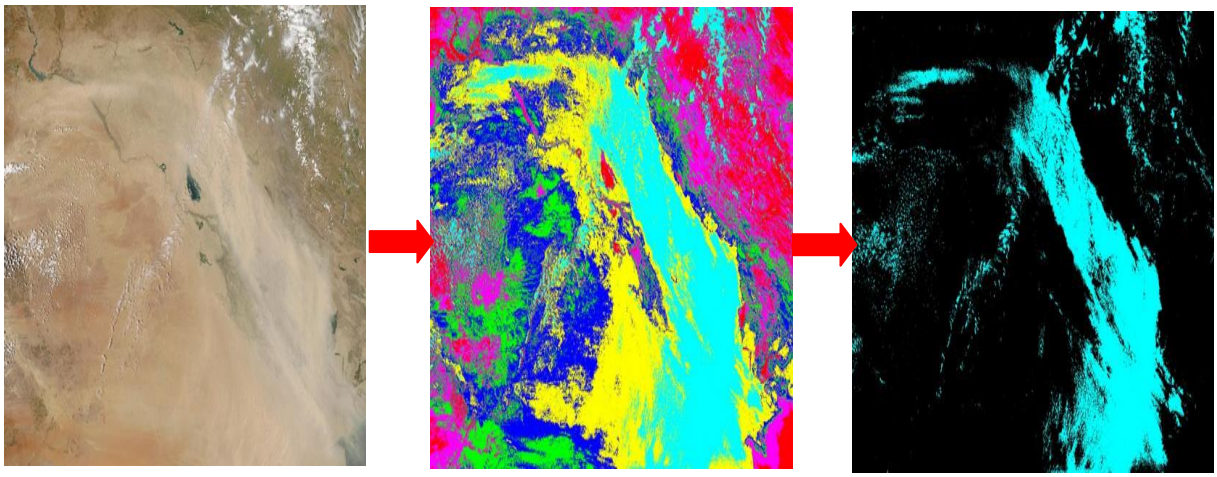

Figure 12- A, true color, B, all classes and C, the dust class at 6-7-2010 dust class No. 5

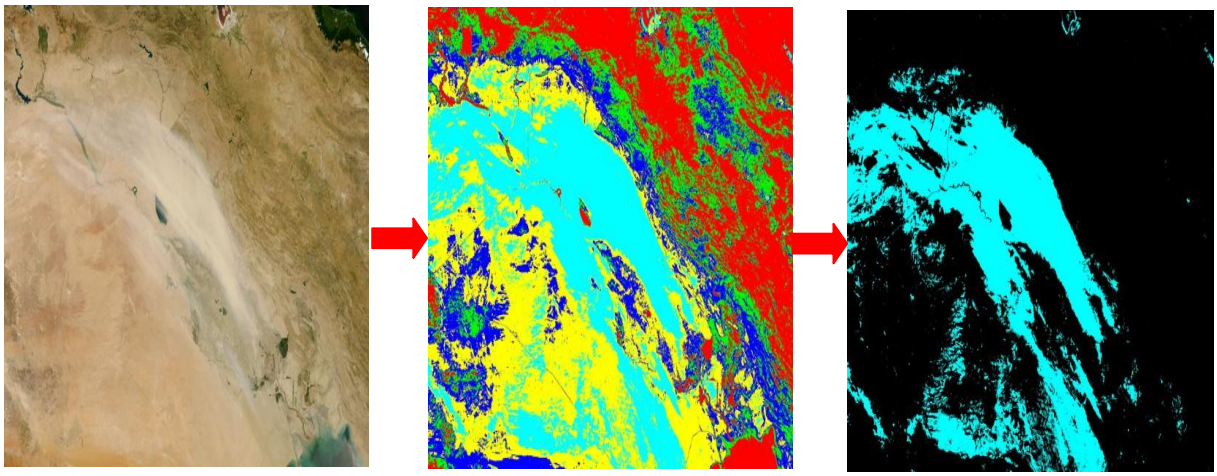

Figure 13- A, true color, B, all classes and C, the dust class at 21-7-2010 Dust class No.6

Table 5- The Percentage Class Distribution

Date	Class 1	Class 2	Class 3	Class 4	Class 5	Class6
6-7-2010	8.424%	13.905%	21.218%	23.348%	18.500%	14.605%
21-7-2010	0	22.067%	13.179%	15.415%	26.972%	22.368%

Table 6- represent 3 dust storms and their points of its generation

Point	22/2/2010 Yellow		6/7/2010 Cyan		21/7/2010 Red	
	Lat.	Long.	Lat.	Long.	Lat.	Long.
Point1	35˚15′81″	38˚04′87″	40˚16′17″	39˚04′02″	34˚55′63″	43˚27′14″
Point2	35˚29′56″	38˚34′91″	39˚16′86″	39˚13′31″	35˚40′99″	44˚11′18
Point3	35˚39′01″	39˚03′50″	39˚37′84″	40˚24′27″	34˚29′89″	43˚50′33″
Point4	35˚56′24″	38˚51′34″	39˚31′20″	41˚12′42″	35˚20′35″	44˚10′56″
Point5	36˚02′21″	41˚34′00″	40˚04′33″	35˚37′12″	35˚33′48″	44˚11′15″

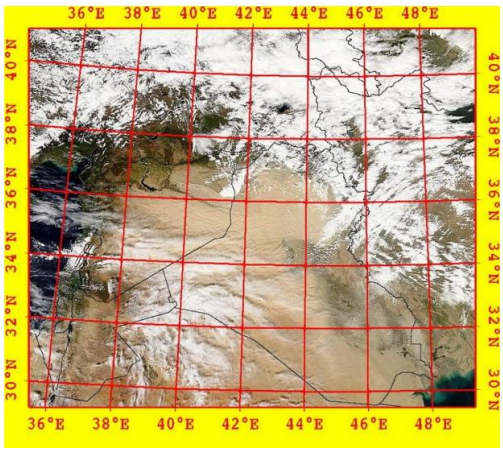

Figure 14- image for Dust Storm 21/7/2010 with map information

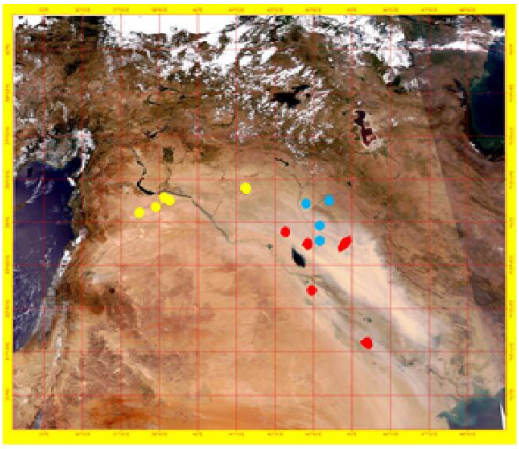

Figure 15- The Dust generation Areas

Table 6- is very important to know the source area with specific coordinate the these point is the center of radius 10 km or more depend on land type (clay, silt and find sand).

Table 7- Covered Area by dust

Dust day	Dimension (Pixel)		Area (Km) for each pixel		Total area (Km^2)
	X	Y	X	Y	
6-7-2010	2754	1761	0.36851	0.48805	872241.7
21-7-2010	2268	1701	0.36973	0.48803	696111

Table 8- Dust Mass Calculation

day	Area of image (Km^2)	Per. of dust (class)	Area of dust (Km^2)	Density (mg/m^3)	Height(Km)	Total dust (Kg)
6-7	872241.7	18.500%	161364	1.58	0.2	50.9×10^6
21-7	696111	22.368	153144.4	1.58	0.2	48.3×10^6

Results Analysis

The dust mass that attack the country was about 100000 tones at July 2010, table 8- . The covered areas by dust was included all the country region, especially in the south and mid, due to the wind direction from north to south. The dust generation areas were located in the Iraq and Syrian, this regions can be runoff by water in order to reduce the dust affect, figure 15- . The dust density value can be detected from the brightness of pixel values, as the brightness increase, the dust density was increase, see figure 15- . The weather parameters temp. Humidity, etc. does not affected the dust palpability, only the rain fail was the major factor. The NDVI dust detection method was simple and yield a good results. The PCA change detector results affected by the images quality, low correlation values between band, yield low change detection. In the classification process, some pixels were added to the dust class due to the interference with cloud pixels, the percentage of interference 5%, figure 12A- .

Conclusions

The main conclusion are All dust storms are generated from north and north-west of Iraq because the wind direction is mainly north and north-west and is called shemal winds. The temperature, humidity and pressure this characteristic do not take place on the dust storms generation because the Iraq weather is all most dry and hot most of the year, but, the rain percentage makes a deference in the frequency of this phenomena .All images resolutions is 250 meter form the MODIS satellite, but, in one scene for each day that is not give more details for the exact area that generate the dust storms. The images may be taken after several hours or more than after dust storm started. The number of classes that obtained to the original images is give the same density for the dust in the images. This problem give some percentage of error in the result. The density used for the result is the same in the two calculations for dust mass and this make the second error for the exact result and this problem can be solved by take dust sample form each day get dust storm. The height

is the same in the calculation and this make the third source of error in the result and can be solve by taking the range of high for the dust storm in the same day that when this phenomena take place. The images and the calculation is made for the same month (July), because of the high frequency of dust storm is rising in the summer and the people get more ventilation because of the height temperature in the summer. That will case more problem for their health

References

1. Mei DI., Xiushan L., Lin S. and Ping W. **2008** "A Dust-storm Process Dynamic Monitoring with multi-temporal Modes' Data", pp.965-968 Geomantic College, The International Archives of the Photogrammetry, *Remote Sensing and Spatial Information Sciences*. Vol. XXXVII. Part B7. Beijing.
2. Merchant C. J., Embury O., Borgne P. Le and Bellecb B., **2006**"Saharan dust in nighttime thermal imagery: detection and reduction of related biases in retrieved sea surface temperature ", *Remote. Sensing. Environ*, pp:15-30.
3. Kaufman Y. J., **1995**"Remote sensing of the direct and indirect aerosol forcing", pp:298-332, in Aerosol Forcing of Climate, Charlson and Heintzenberg, Eds. London, U.K. Wiley,.
4. Alpert P., Kaufman Y. J., Shay Y. -El, Tanre D., Silva A. da, Schubert S., and Joseph Y. H.,**1998** "A first inference of Atmospheric Response to Dust Forcing from a Data Assimilation System", *Nature*, 395, pp:367-370.
5. Charlson R. J., Schwartz S. E., Hales J. M., Cess R. D., Coakley J. A. Jr., Hansen J. E., and Hofman D. J., **1992**"Climate forcing of anthropogenic aerosols ", *J. Science*, 255, pp:423-430.
6. Kaufman Y. J., Tanré D., Remer L., Vermote E., Chu A., and B. Holben N., **1997**"Remote sensing of tropospheric aerosol from EOS-MODIS Over The Land Using Dark Targets and Dynamic Aerosol models ", *J. Geophys Res.*, 102, pp:17051-17067.
7. Michshenko M. I. and Travis L. D., **1997.** "Satellite retrieval of Aerosol Properties Over the Ocean using Polarization as well as Intensity of Reflected Sunlight ", *J. Geophys. Res*., 102, pp:16989-17014.
8. Nakajima T. Y., Fukushima H., Kuji M., Uchiyama A., and Kishino M., **1998.** "Optimization of the advanced earth observing satellite II global imager channels by use of radiative transfer calculations ", *Applied Optics*, 37, pp:3141-3163.
9. Kahn R., West R., McDonald D., Rheingans B., and Mishchenko M. I., **1997** "Sensitivity of multi angle remote sensing observations to aerosol sphericity ", *J. Geophys. Res*., 102, pp:861-870.
10. Merchant C. J., Embury O., Borgne P. Le and Bellecb B., **2006**"Saharan dust in nighttime thermal imagery: detection and reduction of related biases in retrieved sea surface temperature ", Rem. Sens. Environ, pp:115-30.
11. Deschamps P. Y., Bréon F. M., Leroy M., Podaire A., Bricaud A., Buriez J. C., and Sèze G., **1994**"The POLDER mission: Instrument characteristics and scientific objectives ", Geosci. Remote Sensing, 32, pp:598-615.
12. Deuzé J. L., Bréon F. M., Deschamps P. Y., Devaux C., Herman M., Podaire A., and Roujean J. L., **1993**"Analysis of the POLDER (polarization and directionality of earth's reflectance): Airborne instrument observations over land surfaces ", *Remote Sens. Environ*., 44, pp:151-168.
13. Qu J. J., Hao X., Kafatos M., and Wang L, **2006**"Asian dust storm monitoring combining Terra and Aqua MODIS SRB measurements ", *Geosci. Re*. 3, pp:484-485.
14. Gao B. C., **1996**"NDWI–A normalized difference water index for remote sensing of vegetation liquid water from space ", *Remote Sens. Environ*., 58, pp:257-266.
15. Miller S. D.. **2003**"A consolidated technique for enhancing desert dust storms with MODIS ", Naval Research Laboratory, Monterey, California, USA. Geophysical Research 30.
16. C. H. Wash and T. Murphree. **2004**"An Analysis of A Dust Storm Impacting Operation Iraqi Freedom, 25-27 March 2003 ", Naval Postgraduate School, Monterey, California. USA.
17. Hao X., Qu J. J. **2007**"Saharan dust storm detection using moderate resolution imaging spectroradiometer thermal infrared bands ", *Journal of Applied Remote Sensing*, 1, 013510 (24 April).

18. Ackerman S. A., **1997**"Remote sensing aerosols using satellite infrared observations ", *J. Geophysics. Res*. 102.
19. Patterson E. M., Gillete D. A., and Stockton B. H., "Complex index of refraction between 300 and 700 nm for
20. Simond J. L., **1962** "Application of characteristics vector analysis to photographic and optical response data", *Journal of the Optical Society of Americ*a, 53(8), pp:968-975.